

Bismuth doped fiber laser and study of unsaturable loss and pump induced absorption in laser performance

Mridu P. Kalita,* Seongwoo Yoo, and Jayanta Sahu

Optoelectronics Research Centre, University of Southampton, Southampton SO17 1BJ

*Corresponding author: mpk@orc.soton.ac.uk

Abstract: A short Bi doped fiber laser operating in the wavelength region of 1160-1179 nm has been demonstrated. The influence of unsaturable loss on laser performance is investigated. Excited state absorption in Bi doped germano-alumino silicate fiber is reported in the 900-1300 nm wavelength range under 800 and 1047 nm pumping. Bi luminescence and fluorescence decay properties under different pumping wavelengths are also investigated.

©2008 Optical Society of America

OCIS codes: (140.3510) Lasers, fiber; (140.3380) Laser materials; (060.2290) Fiber materials; (060.2310) Fiber optics.

References and links

1. N. S. Sadick and R. Weiss, "The utilization of a new yellow light laser (578 nm) for the treatment of class I red telangiectasia of the lower extremities," *Dermatol Surg.* **28**, 21-25 (2002).
 2. C. E. Max, S. S. Olivier, H. W. Friedman, K. An, K. Avicola, B. V. Beeman, H. D. Bissinger, J. M. Brase, G. V. Erbert, D. T. Gavel, K. Kanz, M. C. Liu, B. Macintosh, K. P. Neeb, J. Patience, and K. E. Waltjen, "Image improvement from a sodium-layer laser guide star adaptive optics system," *Science* **277**, 1649-1652 (1997).
 3. Y. Fujimoto and M. Nakatsuka, "Infrared luminescence from Bismuth-doped silicate glass," *Jpn. J. Appl. Phys.* **40**, L279-L281 (2001).
 4. M. Peng, J. Qiu, D. Chen, X. Meng, I. Yang, X. Jiang, and C. Zhu, "Bismuth- and aluminum-codoped germanium oxide glasses for super-broadband optical amplification," *Opt. Lett.* **29**, 1998-2000 (2004).
 5. X. Meng, J. Qiu, M. Peng, D. Chen, Q. Zhao, X. Jiang, and C. Zhu, "Near infrared broadband emission of bismuth-doped aluminophosphate glass," *Opt. Express* **13**, 1628-1634 (2005).
 6. M. Peng, J. Qiu, D. Chen, X. Meng, and C. Zhu, "Superbroadband 1310 nm emission from bismuth and tantalum codoped germanium oxide glasses," *Opt. Lett.* **30**, 2433-2435 (2005).
 7. E. M. Dianov, V. V. Dvoryn, V. M. Mashinsky, A. A. Umnikov, M. V. Yashkov, and A. N. Gur'yanov, "CW bismuth fiber laser," *Quantum Electron.* **35**, 1083-1084 (2005).
 8. E. M. Dianov, A. V. Shubin, M. A. Melkumov, O. I. Medvedkov, and I. A. Bufetov, "High-power cw bismuth-fiber lasers," *J. Opt. Soc. B* **24**, 1749-1755 (2007).
 9. A. B. Rulkov, A. A. Ferin, S. V. Popov, J. R. Taylor, I. Razdobreev, L. Bigot, and G. Bouwmans, "Narrow-line, 1178 nm CW bismuth-doped fiber laser with 6.4 W output for direct frequency doubling," *Opt. Express* **15**, 5473-5476 (2007).
 10. V. V. Dvoryn, V. M. Mashinsky, and E. M. Dianov, "Efficient Bismuth-Doped Fiber Lasers," *IEEE J. Quantum Electron.* **44**, 834-840 (2008).
 11. G. P. Agrawal, *Nonlinear Fiber Optics*, 3rd ed. (Academic Press, San Diego, 2001).
 12. J. E. Román, M. Hempstead, C. Ye, S. Noh, P. Camy, P. Laborde, and C. Lermiaux, "1.7 μm excited state absorption measurement in erbium-doped glasses," *Appl. Phys. Lett.* **67**, 470-472 (1995).
 13. I. A. Bufetov, S. V. Firstov, V. F. Khopin, A. N. Guryanov, and E. M. Dianov, "Visible luminescence and up-conversion processes in Bi-doped silica-based fibers pumped by IR radiation," in *Proceedings of ECOC 2008*, Brussels, Belgium, paper, Tu.3.B.4.
 14. M. Grinberg, D. L. Russell, K. Holliday, K. Wisniewski, and Cz. Koepke, "Continuous function decay analysis of a multisite impurity activated solid," *Opt. Commun.* **156**, 409-418 (1998).
-

1. Introduction

With the increased amount of data transfer in telecommunication systems, there is a growing interest in finding efficient laser sources or amplifiers in the wavelength region of 1100 – 1500 nm, in order to extend the usable spectral range to the second telecommunication window, which is also the zero dispersion wavelength region of silica fiber. Moreover, the availability of efficient lasers in this wavelength region will allow for the creation of efficient

visible lasers, in particular yellow light sources, by frequency doubling, which is promising for dermatological and astronomical applications [1, 2].

In recent years, a novel luminescent material based on Bi doped silica glass in the 1.3 μm wavelength region has gathered a lot of attention [3-6]. The active centre responsible for the origin of this near infrared luminescence is still unclear and has been assigned to Bi^{5+} [3], Bi^+ [5] or even Bi clusters [6]. Subsequently, the first fabrication and realization of Bi doped fiber laser (BiDFL) action in the range of 1.15 – 1.21 μm was reported, when pumped at 1.06 μm [7]. An increase in the efficiency up to 22%, in the high pump power region, was also reported; however an 80 m long fiber was required for the laser experiments due to its low pump absorption of 0.3 dB/m [8]. Another experiment on a BiDFL, which utilized a similarly low Bi concentration fiber, also used an 80 m long Bi doped fiber (BiDF) [9]. Up to date, the maximum laser efficiency achieved is 32%, when water cooled (20°C), using 55 m long fiber [10]. For reasons such as background loss and nonlinearities, shorter fibers are generally preferred, but it appears that low Bi concentration has prevented progress towards shorter fibers. Indeed, 0.005% of Bi by wt. was set as an upper limit for Bi laser action [9]. There are possibly two challenges in increasing the Bi concentration. First, the desired infrared luminescence is only achievable when the Bi ions sit in proper sites [3]. Hence, increasing the Bi concentration beyond what the number of appropriate sites permit may cause unsaturable absorption or, at best, have no effect. Secondly, as the lasing wavelength is located in the tail of the pump absorption band, high Bi concentration gives rise to additional signal loss like an unsaturable loss. Depending on the excited-state lifetime, this can lead to high thresholds in long devices of high Bi concentration. Despite these challenges, it is imperative to develop efficient, high Bi concentration, fiber for short fiber laser operation and avoid any unwanted nonlinear effects for cladding pumped BiDFL.

In this paper, we report continuous wave lasing operation at 1160 and 1179 nm with ~25 m long BiDF. We discuss the impact of unsaturable loss on Bi laser performances and the intricacy of increasing Bi concentration for reducing fiber length. Furthermore, an opportunity to extend the pump band for the BiDFL was investigated by measuring the excited state absorption (ESA) in BiDFs in the 900-1300 nm wavelength range under 800 and 1047 nm pumping. Dependence of Bi fluorescence on pump wavelength was also investigated.

2. Experimental

A series of BiDF preforms with a core glass composition of Ge:Al:SiO_2 was fabricated by modified-chemical-vapor-deposition (MCVD) and the solution-doping technique with varying Bi, Ge and Al concentrations. The preforms were drawn into fibers with 125 μm outer diameter with higher index polymer coating materials. The characteristics of the fibers are summarized in Table 1.

Table 1. Characteristics of the developed Bi-doped fibers and fiber lasers at room temperature

Fiber number	Absorption at 1080 nm (dB/m)	Absorption at 1160 nm (dB/m)	Background loss at 1285 nm (dB/km)	Estimated Ge content (mol %)	Estimated Al content (mol %)	Unsaturable loss at 1080 nm (dB/m)	Laser efficiency at 1160 nm (%)
Fiber 1	1.2	0.3	40	0.6	1.2	0.4	10
Fiber 2	1.7	0.5	60	0.4	1.2	1.1	< 1
Fiber 3	3.5	1.3	100	Negligible	1.8	2.9	No lasing

2.1 Absorption

Figure 1 shows the typical absorption spectrum in the spectral region of 800-1300 nm, measured by the cut-back technique, using a white light source and optical spectrum analyzer. The small signal absorption at 1080 nm is 1.2 dB/m for fiber 1 which is four times higher than that for the other BiDFs used for the laser operation, fabricated by the conventional MCVD

and solution doping technique [8]. It should be noted that, despite the high absorptions, all the fibers have background loss of less than 100 dB/km at 1285 nm from the OTDR (Luciol) measurements.

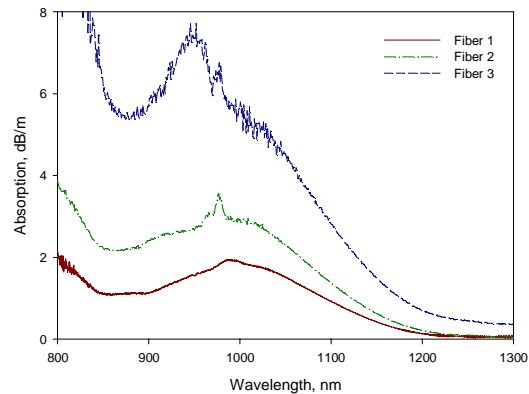


Fig. 1. Measured absorption spectra of the BiDFs.

2.2 Unsaturable loss

The unsaturable losses in all the three fibers were measured at the pump wavelength of 1080 nm, at room temperature. A 3 W Yb doped fiber laser at 1080 nm was used as the pump source. A short length of Fiber 1 was used in order to avoid any undesired gain at the signal band around 1160 nm. The output spectrum was monitored on the optical spectrum analyzer to check the power level in the signal band. The maximum pump power launched into the fiber was ~2.5 W, which was sufficient to saturate the absorption. The unsaturable loss in Fiber 1 was found to be almost 0.4 dB/m, which is 33% of the total small signal absorption measured at this wavelength, as shown in Fig. 2.

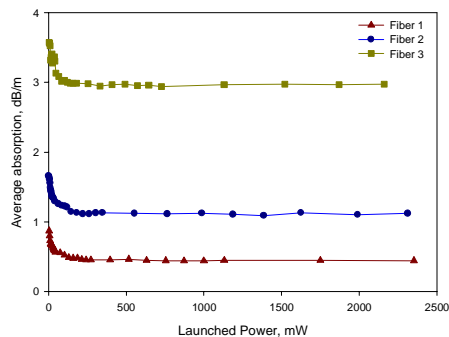


Fig. 2. Average absorption of BiDF against launched power at 1080 nm.

In Fiber 2, the unsaturable absorption was 1.1 dB/m which is 64% of the total small signal absorption measured. Fiber 3 revealed an unsaturable absorption of 2.9 dB/m, which is 82% of the total Bi induced absorption measured at this wavelength. The unsaturable loss in BiDF increased at a shorter wavelength of 1047 nm, and decreased at lower temperature (10°C), which is in good agreement with previous results [8, 10]. Note that we did not observe any temperature dependence of the small signal absorption in the wavelength range investigated. This suggests that the reduction in unsaturable loss at lower temperature can be viewed as a suppression of the unsaturable loss part in the measured small signal absorption. Thus, the Bi

laser efficiency would be improved with an externally forced heat sink, or by pumping the fiber with the wavelength possessing lower unsaturable loss.

2.3 Laser Oscillation

The BiDFL configuration for Fiber 1 is shown in Fig. 3. Core pumping of the laser cavity was organized by using a 3 W Yb doped fiber laser at 1080 nm. A linear 4%-100% reflecting cavity was formed by a perpendicularly cleaved end facet in the signal output port of the WDM and a high reflecting broadband mirror butted to the fiber on the other end of the cavity. The fiber length was varied from 50 to 20 m to maximize the signal output power.

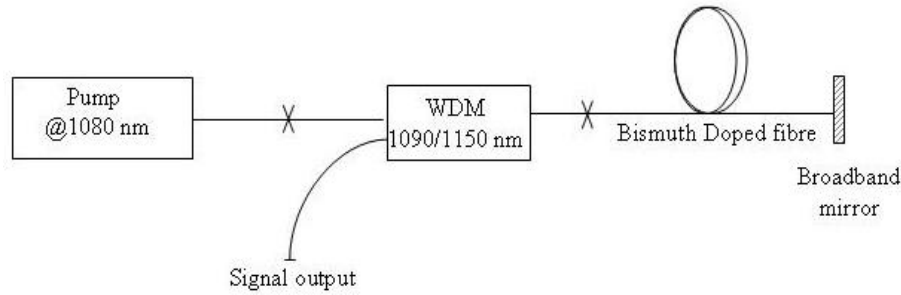


Fig. 3. Experimental arrangement for BiDFL.

The dependence of output laser power on the launched pump power is shown in Fig. 4(a). We attained 10% slope efficiency at 1160 nm with respect to the launched pump power. The fiber length was 25 m which is substantially short compared to other 80 m BiDFLs. The 10% slope efficiency compares well with other reported 80 m long fiber lasers at low pump powers [8]. The lasing threshold was around 200 mW. We observed no pulsing in a 25 m BiDFL. It is worth noting that this short fiber substantially increases the Raman limit up to 2 kW [11], which is important for pulsed operation. Figure 4(b) shows a typical spectrum of 1160 nm BiDFL with a linewidth of 3 nm, which was taken by an optical spectrum analyzer with 1 nm resolution. The broad linewidth is due to the free running laser configuration.

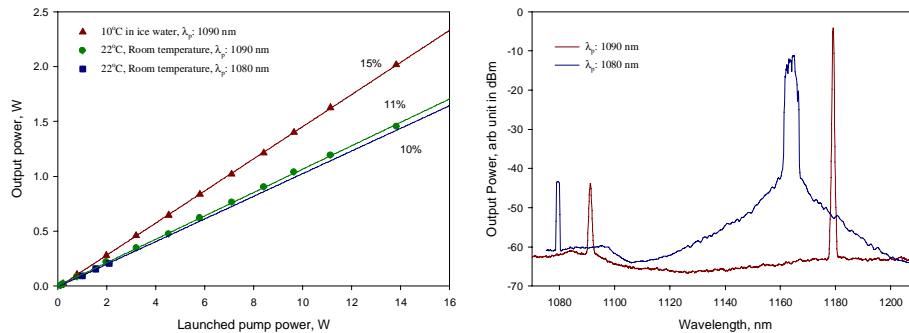


Fig. 4. (a). Output power and (b) output spectrum of BiDFL.

Fiber 1 was also tested with a 15 W Yb doped fiber laser (SPI Laser) at 1090 nm, using a similar set up, as shown in Fig. 3. Here the 1090/1150 nm WDM was replaced with a 1090/1179 nm WDM. In addition, a fiber Bragg grating at 1179 nm with 11% reflectivity was used for the signal output coupling. The laser efficiency was slightly improved with 1090 nm, compared to the efficiency under 1080 nm pumping, at room temperature. However, the efficiency reached 15% when we dropped the environmental temperature to 10 °C. The response of the laser performance to the different pump wavelengths and the different external

temperatures appears to be in accordance with the observed unsaturable absorption. The maximum signal output power at 1179 nm was 1.4 W at 22°C, which increases up to 2 W at 10°C [See Fig. 4(a)]. The narrow linewidth of 0.4 nm could be suitable for successive frequency doubling to yellow [Fig. 4(b)].

Fiber 2 failed to lase in the 100%-4% linear cavity at room temperature. We tested the fiber in a ring cavity with 65% output coupling. With a 20 m long fiber, when pumped by 1080 nm, the oscillation at 1160 nm was observed, but the efficiency was quite limited to 1%. We checked Fiber 3 in a strong ring cavity with 1% output coupling, but it failed to lase with the available pump power.

The measured value of the BiDFL efficiency, even with the most efficient fiber, is lower than the conventional rare-earth doped fiber lasers. One of the possible reasons for the poor performance of BiDFL may be the presence of unsaturable absorption at the pump wavelength. It should be noted that the laser efficiency indeed relies on the strength of the ratio of unsaturable loss to the small signal absorption. Increasing Bi concentration is certainly the way forward to make the cavity shorter, however, we believe, at least in our fibers, that the higher Bi concentration builds more wrong-valenced or ill-coordinated Bi ions, which restricts the amount of Bi concentration. The unsaturable part in the absorption could be somewhat suppressed by a proper heat sink, as reflected in the BiDFL efficiency in Fig. 4(a). In addition, modification of compositions in host material or different fabrication process may be helpful to reduce the unsaturable loss in BiDFs.

2.4 Excited state absorption

We further investigated the possibility of extending the pumping band of the BiDFs as Bi ions in silicate glasses show a broad and intense absorption band (See Fig. 1). We aimed to reveal the existence of the ESA by measuring change in transmission with and without bleaching the ground state population. The experimental configuration for the ESA measurement in the BiDFs is shown in Fig. 5(a). Chopped white light from a tungsten lamp was launched into one end of the BiDF. The transmitted signal was collected, passed through the monochromator and finally detected with an InGaAs detector. The lock-in amplifier was synchronized with the chopper such that only signal in-phase was collected. An 800 nm Ti:Sapphire laser served as a pump source. Pump light was coupled into the fiber through a dichroic mirror (DM). Saturation in the change in transmission could be observed over 150 mW of the launched pump power. A small signal ground state absorption (GSA) was determined by the cut-back method between fiber lengths 2 and 0.8 m with the pump off. The measured GSA agreed well with the same measurement done with an optical spectrum analyzer and white light source configuration.

The measured change in transmission is determined by [12],

$$\Delta T = -\frac{1}{L} \ln \left(\frac{T_{on}}{T_{off}} \right) = N' (\sigma_{esa} - (\sigma_{gsa} + \sigma_e)) \quad (1)$$

where L is a fiber length, T_{on} and T_{off} are signal transmission with pump on and off, respectively. N' is a constant accounting for the overlap between the signal and the population in the excited state, and σ_{esa} , σ_{gsa} , and σ_e are cross-sections of excited state absorption, ground state absorption, and emission, respectively. It should be noted that ESA was only considered, and other factors like unsaturable loss was ignored in our calculation. Equation (1) suggests that the ESA is dominant over the sum of σ_{gsa} and σ_e when $\ln(T_{on}/T_{off})$ is negative, i.e., when the transmission decreases with the pump turned on. The GSA and change in the transmission are shown in Fig. 5(b).

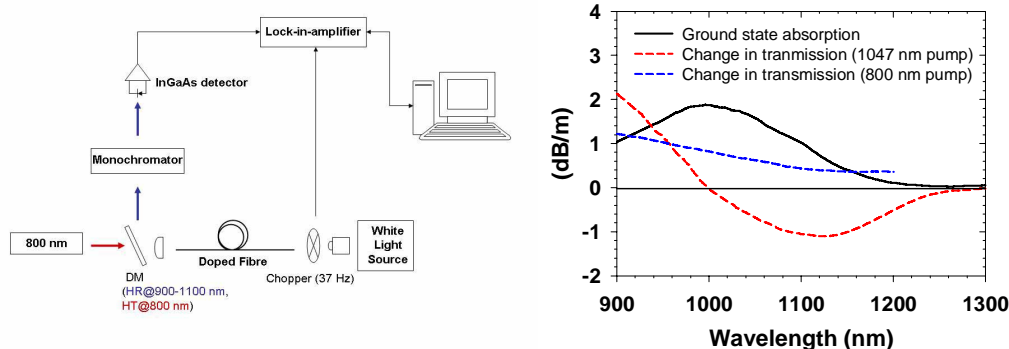


Fig. 5. (a). Experimental set up for ESA measurement under 800 nm pumping and (b) measured ground state absorption and changes in transmission in BiDF output spectrum under 800 and 1047 nm pumping.

Under 800 nm pumping, the ESA is seen to be dominant all over the wavelengths investigated including the Bi emission band. Although the curve of transmission change did not extend to 800 nm, because of the limitation in the DM that covers the 900 nm to 1200 nm range, an increase in absorption at stronger pump power suggested the presence of ESA at 800 nm. The signal ESA on top of the pump ESA makes 800 nm pumping less promising.

The existence of the ESA of the BiDF was also measured under 1047 nm pumping. We used the same experimental arrangement as in Fig. 5(a) except that the DM was replaced by a fiber coupler. A 1047 nm Nd-YLF laser diode was used as a pump source. Counter propagating pump light was injected to the BiDF through the fiber coupler. Fiber lengths 2.7 and 1 m were used for the measurement. The change in transmission is shown in Fig. 5(b). On the contrary to the 800 nm pumping, a strong ESA can only be seen at wavelengths shorter than 1000 nm. Our measurement at 1047 nm pumping showed no significant ESA at the lasing wavelength and also in the 1080 nm pumping band of BiDF. Similar trends were observed in case of Fiber 2 and Fiber 3, when examined under 1047 nm pumping. It should be mentioned that we only consider ESA and neglect other possible causes of pump induced absorption like up-conversion as reported in [13].

2.5. Fluorescence dependence on pump wavelength

We further investigate the fluorescence dependence on the pump wavelengths. Figure 6 presents the measured fluorescent spectra for Fiber 1 at different pumping wavelengths from 915 to 1090 nm. Note that the peaks were scaled to unity for comparison. The fluorescence peak shifts towards longer wavelengths and become narrower with longer pump wavelengths. We observed similar pump wavelength dependence of fluorescence in other fibers.

The fluorescence decay time also depends on the pumping wavelengths. The recorded time of the Fiber 1 was 750 μsec under 1090 nm pumping, but it reduced to 670 μsec under other pump wavelengths of 915 and 976 nm [Fig. 7(a)]. The observed lifetimes of Fiber 2 and Fiber 3 under 1090 nm pumping were 750 μsec , which reduced to 680 μsec under 976 nm pump wavelength. No temperature dependence on lifetime was observed at the temperature range of 10 to 22°C, in all the three fibers measured. We resolved the measured decay curves with continuous lifetime fitting to recover all possible decay constants as in [14]. The decay curves revealed two different decay constants. For example, the decay curve of the Fiber 1 showed short and long decay times of 130 μsec and 750 μsec respectively, at 1090 nm pumping. The decay curves were fitted with single exponential and continuous life time distribution fit, and they were all better expressed by continuous exponential fitting, as shown in Fig. 7(b).

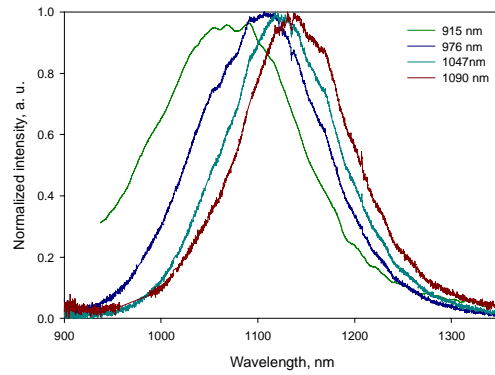


Fig. 6. Scaled fluorescence spectra of Fiber 1 by different excitation sources.

Thus, it seems to indicate that the Bi ions, which are responsible for 1160-1300 nm emission, do sit in different sites.

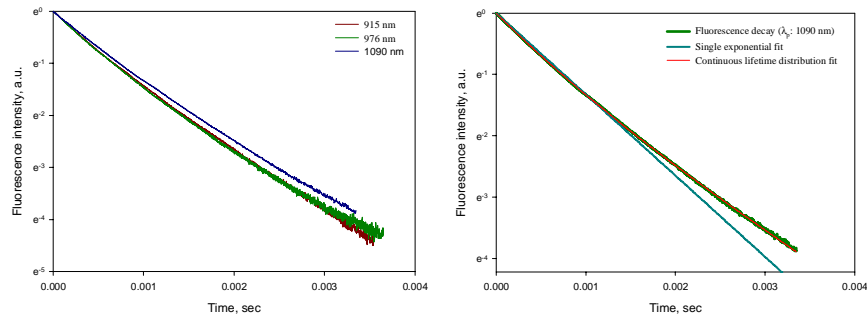


Fig. 7. (a). Fluorescence decay of BiDF under 915, 976 and 1090 nm pumping and (b) fluorescence decay fitted with single and continuous life time distribution under 1090 nm pumping.

3. Conclusion

We have demonstrated a 25 m BiDFL at 1160 nm. The laser efficiency was impaired when unsaturable loss was high. The temperature dependence of unsaturable loss and its influence on the efficiency of BiDFL operation was investigated. The ESA in BiDF was measured in the 900 – 1300 nm wavelength range under 800 nm and 1047 nm pumping. The measurement under 800 nm pumping revealed strong ESA from 900 – 1200 nm. Strong pump ESA together with the observed signal ESA will obstruct efficient laser performance by 800 nm pumping. Under 1047 nm pumping, a significant amount of ESA was observed in the 900 – 1000 nm band, while the ESA in the Bi emission band was negligible. The fluorescence of the BiDF strongly depends on the pump wavelength.

Acknowledgment

The authors would like to thank Christophe Codemard and Carl Farrell (Optoelectronics Research Centre, University of Southampton) for their valuable help.